의학박사 학위논문

신경재생의 정합성 향상을 위한 혈소판 풍부혈장 탑재 신경도관 개발

Development of nerve guide conduit eluted platelet-rich plasma for reduction of axonal mismatch in neural regeneration

울산대학교 대학원

의 학 과

김 지 원

신경재생의 정합성 향상을 위한
혈소판 풍부혈장 탑재 신경도관 개발

지도교수 최승호

이 논문을 의학박사 학위 논문으로 제출함

2020년 2월

울산대학교 대학원
의 학 과
김지원

김지원의 의학박사학위 논문을 인준함

심사위원 이 윤 세 (인)

심사위원 최 승 호 (인)

심사위원 김 상 윤 (인)

심사위원 심 봉 섭 (인)

심사위원 최 정 석 (인)

울 산 대 학 교 대 학 원

2020 년 2 월

국문요약

배경: 갑상선 절제술 중 되돌이 후두 신경(recurrent laryngeal nerve, RLN)은 쉽게 손상될 수 있으며, 이로 인해 발생한 성대 마비는 쉰 목소리, 흡인성 폐렴 및 호흡 곤란을 일으키며, 생명을 위협 할 수도 있다. 이에 저자는 이러한 되돌이 후두신경 손상시 기능적 신경 재생을 위한 혈소판 풍부 혈장 (platelet rich plasma, PRP)을 함유하는 다공성 폴리카프로락톤 신경 유도 도관 (Nerve guidance conduit, NGC)의 유용성을 세포 실험 및 동물 실험으로 평가하였다.

방법: 인간 슈반 세포주에 PRP 를 처리 한 후 세포 증식, 이동을 평가 하였고, RT PCR 및 웨스턴 블롯으로 신경 자극 인자, 수초 관련 당 단백질 (MAG) 및 ERK 의 발현을 확인하였다. 동물실험으로는 22 마리의 뉴질랜드 흰 토끼에서 왼쪽 RLN 의 10mm 세그먼트를 절제하고 두 그룹(일반 NGC = 10 마리, PRP 가 탑재된 NGC = 12 마리)으로 나누어 성대의 움직임, 조직 등을 관찰하였다. 성대의 기능적 움직임은 수술 후 8, 12 및 16 주에 내시경을 이용하여 동적 평가를 시행하였고, 성대근육의 위축 및 도관내 재생된 신경의 길이, 성분 등은 H&E 및 톨루이딘 블루 염색에 의해 평가하였다. 도관내 재생된 조직은 아세틸콜린 에스테라제 (AchE), 뉴로필라멘트 (NF) 및 항-S100 단백질에 대한 면역 조직 화학적 염색 및 전자현미경 분석을 수행 하였다.

결과: 세포 실험 결과, 슈반 세포의 증식, 이동은 PRP 농도에 비례해서 증가 하였다. PRP 농도가 증가할수록 신경 자극 인자, MAG 및 ERK 의 발현이 증가하였다. 동물실험 결과, 내시경 평가상 일반 NGC 그룹보다 PRP 가 탑재된 NGC 그룹에서 유의하게 더 우수한 신경 회복을 보여 주었다. PRP 탑재 그룹은 순수한 PCL 그룹보다 성대 근육의 면적 비율이 상당히 높고 위축이 적었으며, 신경 말단에서 AchE, NF 및 S-100 의 발현이 유의하게 더 강하였다. 신경말단에 조직학적으로 두 신경 말단에서 조직학적으로 신경 성장이 더 조밀하게 관찰되었다. 전자현미경에서도 PRP 탑재 NGC 그룹에서 보다 밀도가 높은 수초화된 축삭을 관찰할 수 있었다.

결론: PRP 가 분비하는 신경자극인자는 그 자체로 슈반세포의 증식과 발현 및 재생을 촉진 시키며, PRP 는 슈반세포의 신경자극인자 분비를 증진시킨다. 생체 내에서도 PRP 탑재 NGC 는 일반 NGC 보다 더 나은 신경 재생결과를 보였다. PRP 탑재 NGC 는 되돌이 후두 신경 재생에 유리한 환경을 제공하고, 말초 신경 손상에 대한 잠재적 치료제가 될 수 있을 것이다.

중심단어: nerve guidance conduit, platelet-rich plasma, nerve, regeneration

목 차

그림 목차

Introduction

During the thyroid and thoracic surgery, recurrent laryngeal nerve (RLN) can be resected or damaged, which results in vocal cord paralysis (VCP) [1]. VCP shows the symptoms including hoarseness, aspiration, and dyspnea and may even be life-threatening [2]. Therefore, when there were a RLN tumor invasion or its sacrifice and resection, surgeons underwent intraoperative reconstruction of the transected RLN [3]. The surgical options include the intraoperative RLN primary repair (end to end epineural suture) and autogenous nerve transplantation to repair the injured nerves [4, 5]. However, primary repair method could apply for the cases that RLN defect was 5 mm or less, and both stumps could be approximated without tension. Furthermore, donor site defect is inevitable in the procedure of autogenous nerve transplantation, and morbidity including neuroma formation, fascicle mismatch, and scarring [6]. Even though the stumps of RLN well connected, it often happened the axonal mismatch, the deprivation of mature neurons proliferation which results in target muscle atrophy, the function restoration are not yet satisfactory [2, 7]. It is now important to develop more applicable approaches for the repair of RLN injury for the functional recovery of vocal cord.

Basically, regeneration of the peripheral nervous system (PNS) injury has a better outcome compared to the central nervous system (CNS). In mammalian PNS, axonal outgrowth exists and substantial functional recovery can occur whereas CNS injury results in a glial scar that inhibits neural growth [8]. There are several researches a more optimal environment for peripheral nerve regeneration [9-13]. The most commonly studied methods include: stem cells, and growth factors containing or eluding materials delivery to stimulate regenerating axons and implanting nerve guidance conduits (NGC) and scaffolds at injury site [6].

Previous study developed an asymmetrically porous membrane manufacturing with polycaprolactone (PCL)/Pluronic F127 that contains the different pore size between inner (nano-sized) and outer (micro-sized) surface [14]. It has selective permeability, that cannot permit the inflammatory cell and myofibroblast migration into inner side of tube, but allows the permeation of nutrients/oxygen, which is critical component for effective nerve regeneration through a NGC [15]. The efficacy of NGC system with different surface pore

structures seems to be verified in a rat sciatic nerve defect model [14] and RLN defect model [2]. Recently, tissue engineered conduit developed the strategies to help axonal sprouting such as neurotrophic factors, growth factor and stem cells release. Platelet-rich plasma (PRP) contains various growth factors and appears to have the potential healing effects on tendon, ligament, muscle, bone and peripheral nerve regeneration [16, 17]. PRP includes several growth factors (GFs), the effect of these GFs on nerve regeneration has been studied [18]. However, the evidence is lack regarding its biological effect of PRP on Schwann cells (SCs) [15].

The aims of this study were to evaluate the ability of PRP loaded NGC for peripheral nerve regeneration compared to non-filled NGC (Fig.1A and B) and to demonstrate whether PRP might modulate the cellular proliferation, neurotrophic function and migration behaviors of SCs (Fig. 2A,B and C).

2. Materials and methods

2.1. Preparation and quantification of PRP

We used pure PRP prepared from blood of rats according to the procedure by adapting the protocol proposed by Sonnleitner et al.[19] The collected blood was firstly centrifuged at 160 G, for 20 minutes, at environmental temperature (22ºC). Then, we pipetted upper straw-yellow turbid fraction and transferred to other 5 ml vacuum tube. The sample was then submitted to a new centrifugation at 400 G, for 15 minutes, resulting in two components: one upper layer on the tube (platelet-poor plasma, PPP) and other lower layer the tube (PRP). PRP were pipetted and transferred to different sterile dishes, they were activated by 0.05 ml of 10% calcium chloride solution (ScienceLab.com Inc., Houston, TX, EUA) to each 1 ml of PRP. PRP was activated before insertion into the wells by adding 1ml of each preparation to 50µl of calcium gluconate and 50µl autologous thrombin. For the quantification of PRP, we detected the platelet activation marker CD62 by fluorescence-activated cell sorting (FACS), and measured the concentration of transforming growth factors- beta (TGF-β) secreted from PRP.

2.2. Characteristics of NGC

Asymmetrically porous PCL/F127 NGCs with selective permeability were prepared by rolling an asymmetrically porous sheet fabricated using an immersion precipitation method, as previously described [14]. Briefly, to prepare an asymmetrically porous PCL/F127 sheet (nano- and micropores on both surfaces), PCL pellets were dissolved in tetraglycol (12 wt%; Sigma Aldrich, St Louis, MO) at 90 ºC, and then Pluronic F127 powder (BASF, Ludwigshafen, Germany) was added in the PCL solution (5 wt%, PCL base). The PCL/F127 solution was filled in a mold (50mm x 50mm x 0.4mm) and immersed in excess water for one hour at room temperature. The precipitated PCL/F127 sheet was washed in excess water to remove the residual tetraglycol. The prepared sheet (thickness ~0.4mm) was vacuum-dried. To prepare the NGC using the asymmetrically porous PCL/F127 sheet, the sheet was rolled into a tube using a 1.5-mm diameter metal mandrel (inside of the tube, smaller pore side) and the edge fold of the sheet was fixed using a tissue adhesive (Histoacryl; B. Braun, Melsungen, Germany). The prepared asymmetrically porous NGCs had an inner diameter of ~1.5mm and a length of ~12 mm.

2.3. PRP containing NGC

Calcium gluconate (0.2 mL, 10%) was added to final 2 ml PRP samples, which were prepared by 2-step centrifugation condition having highest recovery ratio, and the volume of platelet gel was measured at 24 hours with Gelling test [20]. Collagen were added to make the platelet gel. We filled the PRP gel inside the NGC tube using 21G syringes.

2.4. In vitro regeneration study

2.4.1. Preparation for Schwann cells

We used the human Schwann cells (hSCs), purchased from ScienCell Research Laboratories (catalog no.1700; Carlsbad, CA, USA). The cells were cultured in Schwann cell medium (ScienCell Research Laboratories, catalog no.1701, Carlsbad, CA, USA). hSCs were cultured to 85% confluent in the well of 6-well plate. Medium was removed and 1.5 mL of SCM base medium containing CellTracker Green CMFDA (10 μM) was added to each well and incubated at 37°C for 45 minutes. Labeled cells were trypsinized and counted. 1×10^5 hSCs were spun down and resuspended to 200 μL of SCM.

2.4.2 Cell proliferation

Primary SCs were seeded in 24-well plates at a density of 1×104 cells per well, and cultured in DMEM supplemented with 1% FBS (1% FBS/DMEM) (Control group), SC-CM or 1% FBS/DMEM supplemented with PRP at various concentrations (0%, 5.0%, 10%). Cell viability was evaluated by a tetrazolium salt-based assay using a WST-1 Cell. Proliferation Assay Kit (Molecular Probes of Life Technologies Co., Norwalk, CT) on days 1 and 3. The absorbance of soluble formazan was measured at 440 nm with a microplate reader (Molecular Devices). For the cell cycle assay, cells were fixed with chilled 70% ethanol at − 20 °C overnight after being cultured for 5 days as above. The fixed cells were centrifuged, washed and stained with propidium iodide (PI) dissolved in RNase buffer (BD PharMingen, San Jose, CA) in the dark at 4°C for 1 h. The cell count at each phase of the cell cycle was analyzed by flow cytometry (BD PharMingen)

2.4.3. Cell migration and wound healing assay

Cell migration assay was done with transwell assay (Corning Inc, Corning, NY, USA) (Mantuano et al., 2008). The membrane of each insert was coated with fibronectin (Sigma). SCs were planted in the top chamber with Dulbecco's modified Eagle's medium. The lower chambers contained the different concentration (0 and 5%) of PRP gel. After 4 and 8 hours, the migrated SCs were fixed with methanol and stained with crystal violet solution. The non-migrated cells in the upper chamber were wiped with cotton swabs. Migrated cells were imaged and tallied using a DMR inverted microscope (Leica, Mannheim, Germany). The migrated cell numbers were calculated, taking the average number of migrated cells in control group as 100%.

The migratory behavior of the cells was also evaluated by means of a wound healing assay using manual scratching. The scratch assay is a straightforward and economical method used to observe cell migration. Schwann cells were grown to build a confluent monolayer after seeding in the media containing the different concentration (0, 5, and 20%) of PRP gel. Then we performed the scratch using a sterile pipette tip of approx. 500μm. After 4 and 8 hours, the migration rate into this "wound area" was documented and

measured using an inverse Wilovert I microscope (Hund GmbH, Wetzlar, Germany). The migration rate of untreated cells was set to 100% and was compared with cells treated with PRP. Each analysis was performed in triplicates.

2.4.4. Protein expression

Western blot were performed to assess the changes in the hSCs coculture according to the PRP concentration. Primary antibodies are as follows: Myelin-associated glycoprotein (MAG, Santa Cruz Biotechnology, Santa Cruz, CA,U.S.A.), Myelin basic protein (MBP, Santa Cruz Biotechnology, Santa Cruz, CA, U.S.A.), Neurotrophin-3 (NT-3, Santa Cruz Biotechnology, Santa Cruz, CA, U.S.A.), Nerve growth factor (NGF, Santa Cruz Biotechnology, Santa Cruz, CA, U.S.A.) and ERK (Santa Cruz Biotechnology, Santa Cruz, CA, U.S.A.) GAPDH was used to normalize target proteins. Quantitative analysis were were carried out with ImageJ software (version 1.49; Wayne Rasband, National Institutes of Health). To rule out the expression of NGF by rat PRP by itself, NGF concentrations in hSC-media were measured by NGF human ELISA (Abnova, Taipei, Taiwan) according to the manufacturer's protocol.

2.5. In vivo nerve regeneration study

2.5.1. Rabbit recurrent laryngeal nerve injury model

This study was approved by the Animal Ethics Committee of Inha University Hospital (INHA 18 0503-560) and the animals were cared for in accordance with established institutional guidelines. Twenty two female New Zealand white rabbits were used in this experiments. Rabbits were assigned randomly to two groups: pure NGC tube interposed group (n = 10) or PRP containing NGC tube interposed group (n = 12). Right RLNs of all rabbits were preserved as control group, and the left RLN were resected and interposed by NGC (Fig.3A). The animals were subcutaneously premedicated with 0.05 mg/kg glycopyrrolate and 5 mg/kg xylazine, and then anesthetized with an intramuscular injection of 15 mg/kg zolazepam, with all efforts made to minimize suffering. A vertical skin incision was made, followed by division of the platysma and strap musculature. The left RLN was carefully exposed and dissected circumferentially under an operating microscope (Fig. 3B).

A 10-mm segment of the RLN was transected using microscissors. NGCs were interposed between the proximal and distal stumps using two sutures (7-0 vicryl; Ethicon, Somerville, NJ) at each junction (Fig. 3C). The animals were then subjected to one of the following two procedures: (i) nerve resection and NGC tube interposition, or (ii) nerve resection and PRP containing NGC tube interposition. Following the implantation, the muscle incision was closed using a 4-0 vicry (Ethicon), and the skin was closed using a 3-0 ethylon suture (Ethicon).

2.5.2. Evaluation of vocal cord movements

We performed the functional evaluation of RLN. Vocal cord movements were evaluated under an endoscopy laryngeal recording system at 8,12 and 16 weeks postimplantation. The mean relative gap ratio between vocal cord adduction and abduction of the injured vocal cord to the normal side was measured. Endoscopic examinations of vocal cord movement. We captured images of adducted position after nerve stimulation and abducted position. Mean gap ratio during vocal cord movements were significantly different between PRP loaded group and the pure NGC group.

2.5.3. Histological examination

After evaluating vocal cord movement, the animals were euthanized, the RLNs between the proximal and distal stumps were harvested to evaluate nerve growth, and the larynges were excised to assess TA muscle status. RLNs and larynxes were immediately placed in 4% paraformaldehyde at room temperature, processed, embedded in paraffin, and sectioned at 4 lm (RLNs were sectioned longitudinally, and larynxes were sectioned axially). For evaluation, the RLNs were stained with toluidine blue and hematoxylin and eosin (H&E), and the larynges were stained with H&E. The vocalis muscle was evaluated at the level of the vocal process. Muscle sections were observed under a light microscope (Nikon, Tokyo, Japan), and under blinded conditions, a single observer measured the total cross-sectional areas of the muscles. The cross-sectional areas of the vocalis muscle were measured using Image J software by tracing the outlines of the microscopic images. Histologic changes in vocalis muscles were evaluated by calculating the ratios of the areas of denervated vocalis

muscles and the contralateral normal sides (relative area ratios). We calculated the area ratios of vocalis muscle (left experimental area/right normal contol area x 100).

2.5.4. Immunohistochemical analysis

The sections were washed in phosphate buffered saline (PBS; pH *7.4) and pre-incubated for one hour in a blocking solution containing 5% normal goat serum in PBS. After a brief PBS wash, primary antibodies for neurofilament (NF, Thermo Fisher Scientific,) and S100 protein (Merck Millipore, Darmstadt, Germany) diluted in blocking solution were applied. Sections were then incubated overnight at 4C, in secondary antisera (Zymed Laboratories Inc., San Francisco, CA) for 90 minutes at room temperature, and then treated with avidin–biotin–peroxidase solution. The peroxidase label was visualized using diaminobenzidine as the chromogen (Vector Laboratories, Burlingame, CA). Sections were then washed, allowed to air dry, coverslipped, and processed for observation under a confocal microscope (IX81, Olympus, Center Valley, PA). To evaluate the nerve endplates of the regenerated nerves, acetylcholinesterase (AchE) immunohistochemical staining was performed. Briefly, sections were hydrated in water, placed in sodium sulfate solution (20%) for five minutes, rinsed in water, and incubated in acetylcholinesterase solution for up to three hours at 37ºC until bright blue endplates could be clearly distinguished (13). The endplates of the regenerated nerves were evaluated by calculating the ratio of the numbers of injured left and normal right nerve endings.

2.5.5. Transmission electron microscopy evaluation

The regenerating RLNs within NGCs were immersed for two hours in 2.5% glutaraldehyde in 0.1M phosphate buffer (pH 7.4), washed in 0.1M cacodylate buffer (pH 7.4), and postfixed for 90 min in 1% osmium tetroxide containing 0.8% potassium ferrocyanide and 5 nM calcium chloride in 0.1M cacodylate buffer (pH 7.4). Segments were then washed in 0.1Mcacodylate buffer (pH 7.4), stained in 1% uranyl acetate, dehydrated using an acetone series, infiltrated with Poly/Bed 812 resin, and polymerized at 60C for two days. Transverse sections (70nm thick) were obtained using an ultramicrotome (MT-6000-XL-RMC, Boeckeler Instruments, Inc., Tucson, AZ), placed on copper grids, treated with 5%

uranyl acetate and 1% lead citrate, and examined under a transmission electron microscope operated at 80 kV (Zeiss, Oberkochen, Germany).

2.6. Statistical Analysis

All analyses were performed using GraphPad Prism 5.0 (GraphPad Software, Inc., San Diego,CA). The Mann–Whitney test was used to compare the vocal cord movements, the crosssectional areas of TA muscles, and the numbers of nerve endings in the pure NGC tube and PRP containing NGC tube groups. We evaluated the effect of various PRP concentrations on SC migration by Kruskall Wallis test. Statistical significance was accepted for p-values <0.05. All results are expressed as means – standard deviations (SD).

3. Results

3.1. Preparation and characterization of PRP loaded NGC

We chose the PCL/F127 sheet NGC system for this study due to their biocompatibility, ease of PRP gel packing. Analysis of growth factor concentrations in PRP gel samples revealed that the level of TGF-β were significantly higher than resting state (Fig. 4).

3.2. In vitro PRP effect on hSCs

To explore the in vivo effect of PRP as a stimulator of proliferation, firstly we investigated the effects of PRP on hSCs metabolism at various concentration conditions (0%, 5%, or 10%). As Fig. 5A show, hSCs showed typically spindle shaped aligning and had either bipolar or occasionally multipolar morphology. In the proliferation experiment, as shown in Fig. 5B, the number of SCs increased in a dose-dependent manner. Compared with hSCs cultured with 0% PRP, those cultured with 5% to 10% PRP had significantly higher cell viability on days 3 of culture ($P = 0.001$) indicating that proliferation of hSCs was augmented by addition of PRP at these concentrations.

Furthermore, we compare the cell migration on the various concentration of PRP by transwell assay. While the hSCs in the 5% PRP substrates conditions demonstrated significantly faster cell proliferation rates than without PRP condition at 8 hours ($P = 0.043$)

(Fig.6A and B).

To examine the effects of PRP on the migration of hSCs, a scratch wound healing assay was performed. Higher concentrated PRP treated cells significantly increased the migration rate in comparison with hSCs in the PRP untreated condition. The migration rate of the cells in the 10% PRP group was 4.25-fold greater than that of the cells without PRP group ($P < 0.05$) (Fig.7A and B).

Fig. 8A shows the protein expression of SCs proliferation related proteins according to the concentration of PRP. Under the environment of higher concentration of PRP, the neurotrophic factors including NGF and NT-3 showed higher expression compared to the condition of no treatment. Expression of MAG and MBP were increased by PRP dose dependent manner. ERK, which is the MAG related axon cytoskeleton protein, also showed the higher expression when the PRP is administered (Fig. 8B and C). Fig.8D demonstrated the expression of NGF from hSC by human ELISA, hSCs have expressed the NGF in a PRP dose dependent manner.

3.3. in vivo effect of PRP loaded NGC

Endoscopic image of vocal cord movement was analyzed at 8,12, and 16 weeks. Recovery of vocal cord movement were not seen at eight weeks in both groups. At twelve weeks postimplantation, the restoration of vocal cord movement was seen in 1 of 3 (33.3%) rabbits in the pure NGC group and 2 of 4 (50%) in the PRP loaded NGC group. The mobility of vocal cord at sixteen weeks postoperatively were identified in 2 of 4 (50%) rabbits in the pure NGC group and 4 of 5 (50%) in the PRP loaded NGC group. We calculated the relative gap ratios between vocal cord adduction and abduction (Fig. 9A), it showed significantly higher gap ratio in PRP loaded PCL group (80.23 ± 6.91%) compared to the pure PCL group (48.99 ± 10.71%) (P = 0.018) (Fig. 9B)

In terms of target muscle atrophy, we compared the muscle thickness from cross sectional vocalis muscle between groups (Fig.9C). Axial section of vocalis muscle, PRP showed similar muscle thickness at both side, but pure PCL group showed atrophied muscle at left side vocal cord. On quantification analysis, PRP loaded group represented a significant higher area ratios of vocalis muscle (89.34 ± 6.23%) than the pure PCL group

(83.20 ± 6.31%) (P = 0.033) (Fig. 9D).

Longitudinal sections along with RLN at 8, 12, and 16 weeks postimplantation showed gradual nerve growing within NGC. A short structural segment from both stump was found in PRP filled NGC but not in the pure NGC group at eight weeks, and we found the long nerve budding to other side at 16 weeks in PRP loaded PCL group, therefore, RLNs are completely regenerated and connected from both stump (Fig. 10A). Immunohistochemistry results confirmed whether the budding structure from both stumps is the neural structure, the expression of NF, S100, and Ach esterase were abundantly expressed in the PRP loaded NGC group, but were not detected in the pure tube group at sixteen weeks after implantation (Fig. 10B).

Transmission electron microscopy of the mid area of the regenerative nerves in the PRP loaded NGC group at sixteen weeks after implantation showed more abundant myelinated fiber formation than pure NGC. The structure of the axon fibers in the PRP loaded NGC group at sixteen weeks showed more dense and well organized with SCs than eight weeks results (Fig.11A and B).

4. Discussion

Nerve is an electrophysiologic and direction-orientated tissue, therefore, guiding conduit to be able to provide a biomimetic micro-environment is necessary to enhance the peripheral nerve regeneration process [21, 22]. Asymmetrically porous PCL provides a proper environment that stimulates nerve growth and rapid axoglial signaling [14] and PCL with inner PRP consisted of biomolecules and GFs participate in several biological processes involved in nerve regeneration. In this study, we evaluated the PRP loaded NGC regenerated the rabbit RLN efficiently compared hollow NGC, and the hSCs-associated mechanism during the nerve regeneration. Even though there are a few report about usefulness of NGC and PRP for nerve regeneration, to our knowledge, this is the first report demonstrating the efficacy of PRP containing PRP.

Alpha granules of platelets contain growth factors with mitogenic and chemotactic characteristics, such as PDGF, TGF-β, IGF-1, FGF and VEGF. The GFs generated by SCs, such as nerve growth factor, brain-derived neurotropic factor, ciliary neurotropic factor and

glial cell line-derived neurotropic factor, are involved in the modulation of recovery. [23] Schwan cells (SCs) have been shown to play a critical and substantial role in peripheral nerve regeneration. Following peripheral nerve injury, SCs proliferate, form a Büngner belt and devour the debris of denatured axons and myelin together with macrophages. At the same time, SCs express and secrete neurotrophic factors including nerve growth factor (NGF), brain-derived neurotrophic factor (BDNF), neurotrophin-3 (NT-3), and neurotrophin-4/5 (NT-4/5), which play neuron-protective and axon-inductive roles. [24] Qin et al. demonstrated that the concentrated growth factor increases SCs proliferation and neurotrophic factor secretion and promotes functional nerve recovery in vivo. [25] Our results also showed, as the dose of PRP increases, the proliferation of SCs increases. On the other hand, following nerve injury, the migration of SCs is the mechanism to support nerve regeneration. [26] The significant effect of PRP on the increased migration of SCs suggested that the neurotrophic factors such as NT-3 and NGF in the PRP play an essential role in the promotion of SCs migration.

Myelin-associated glycoprotein (MAG) is a molecule expressed by myelinating cells at the myelin/axon interface, and helped to establish its critical roles in the normal formation and maintenance of myelinated axons [27, 28] MAG has the ligand that binds an axonal receptor, which activates a signal of cyclin dependent kinase 5 (cdk5) and extracellular signal regulated kinases 1 & 2 (ERK1/2) and greater expression of phosphorylated neurofilaments leading to increased axonal maintenance and survival. [27] Our results showed the PRP enhanced the expression of MAG and myelin basic protein (MBP), a major protein of the myelin sheath [29]. Yao et al demonstrated the Insulin-like growth factor I (IGF-I) treatment up-regulates gene expression of MBP, and IGF-I effects on oligodendrocytes, myelin protein synthesis, and myelin regeneration in an experimental encephalomyelitis model.[30] IGF-I acts as neurotrophic factor for peripheral nerve to promote growth and inhibit neuronal and glial apoptosis. [31] Our results showed the expression of MBP triggering by PRP, probably IGF-I in PRP might have a potential protective effect against neuron death by apoptosis. As we can see in the Fig.2, MAG and MBP is main adhesion and signaling proteins of Schwann cell, and it is important role to make cytoskeleton and packing the neurofilaments consisting of axon. PRP promotes the

axonal growth by the stimulationg regenerating Schwann cells.

In previous study, the PCL/F127 NGC group showed the rapid bridging of the 10-mm nerve gap and neural tissue growing at postoperative eight weeks compared to in the silicone tube group [2]. However, in our study, the at post-implantation sixteen weeks groups showed the neural regeneration are more than the time point of eight weeks. However, according to the axial TEM image, we can find the dense axon bundles in PRP filled NGC group, that suggests that nerve can grow slow and dense in the GFs abundant environment. The significant role played by GFs within the PRP has also been highlighted in a rat brain-spinal cord co cultured system, where the addition of PRP supernatant promoted an increase in the size and number of axons [23].

After peripheral nerve injury, a multicellular and pleiotropic molecular response will be activated. This response interplay with SCs, macrophages, endothelial cells (ECs), and fibroblasts, mainly modulated by injured axons, myelin breakdown products, soluble factors, and hypoxia as main signals [32]. It will end up regrowing and guiding axons, and reconnecting them with the target organs at a rate of about 1 mm per day [33]. SCs show a striking plastic response to the biological battlefield they are exposed to inside a damaged nerve and are the early detectors of damage. In a context- and time-dependent manner, transdifferentiated SCs perform a variety of cell repair tasks from phagocytosing myelin debris to secreting neurotrophic and neurotropic factors (laminin), proliferation and migration, which results in the formation of SC cords and Bungner Bands in the proximal and distal nerve segment, respectively.

However, this study has some limitations. First, the length of the severed RLN in our study was 10-mm, but the maximum length of NGC should be evaluated to determine the proper length for clinical application. Investigation of the applicable maximum length and appropriate timing would be needed. Secondly, we did not compare the efficacy of neural regeneration between the end–to-end epineural suture group and PRP loaded NGC group. However, IKumi et al compared the autologous graft with epineural suture versus autologous graft coated with activated PRP. They found the local PRP administration increases the regenerative axon diameter and axon number at the distal portion. [34] Comparison with the autologous graft with epineural suture would provide sufficient

strength of the regenerative effect of PRP loaded NGC. Thirdly, we did not compare the free growth factored gelatin filled NGC versus PRP loaded NGC. Because we compared the hollow type type NGC in this experiment, therefore further studies with this design will be needed. Finally, we did not check the biocompatiblity and biodegradability of PRP loaded NGC. Evaluation of inflammation and biodegradablitity in the long term period is necessary.

5. Conclusions

In this study, we have demonstrated the therapeutic potential of a NGC system loaded with PRP for nerve regeneration both in vitro and vivo. In terms of the functional regeneration of RLN, PRP loaded NGC is better than pure NGC. PRP loaded NGC group showed the features including lower muscle atrophy, faster nerve growth, and higher well organized axon density. Possible mechanism are SCs migration, wound healing and proliferation. PRP in the NGC would improve the neural cell proliferation and regeneration in the environment of abundant growth factor. Growth factor in PRP increased SCs proliferation by itself and PRP promoted SCs to secrete neurotrophic factors in vitro, and promoted functional recovery after peripheral nerve injuries in vivo. Therefore, PRP loaded PCL/F127 NGC is a promising candidate biomaterial for peripheral nerve regeneration, and may potentially be utilized to repair recurrent laryngeal nerve injuries.

References

[1] G.W. Randolph, The importance of pre- and postoperative laryngeal examination for thyroid surgery, Thyroid : official journal of the American Thyroid Association 20(5) (2010) 453-8.

[2] J.S. Choi, S.H. Oh, H.Y. An, Y.M. Kim, J.H. Lee, J.Y. Lim, Functional regeneration of recurrent laryngeal nerve injury during thyroid surgery using an asymmetrically porous nerve guide conduit in an animal model, Thyroid : official journal of the American Thyroid Association 24(1) (2014) 52-9.

[3] A. Gurrado, A. Pasculli, A. Pezzolla, G. Di Meo, M.L. Fiorella, R. Cortese, N. Avenia, M. Testini, A method to repair the recurrent laryngeal nerve during thyroidectomy, Canadian journal of surgery. Journal canadien de chirurgie 61(4) (2018) 278-282.

[4] J. Ma, T. Sui, Y. Zhu, A. Zhu, Z. Wei, X.J. Cao, Micturition reflex arc reconstruction including sensory and motor nerves after spinal cord injury: urodynamic and electrophysiological responses, The journal of spinal cord medicine 34(5) (2011) 510-517.

[5] S.-C. Zhang, Y. Ma, H. Liu, X. Zhang, Y. Pan, X. Zheng, Intradural lysis and peripheral nerve implantation for traumatic obsolete incomplete paralysis, Surgical technology international 15 (2006) 276-281. [6] M.B. De la Rosa, E.M. Kozik, D.S. Sakaguchi, Adult Stem Cell-Based Strategies for Peripheral Nerve Regeneration, Advances in experimental medicine and biology 1119 (2018) 41-71.

[7] Y. Pan, G. Jiao, J. Yang, R. Guo, J. Li, C. Wang, Insights into the Therapeutic Potential of Heparinized Collagen Scaffolds Loading Human Umbilical Cord Mesenchymal Stem Cells and Nerve Growth Factor for the Repair of Recurrent Laryngeal Nerve Injury, Tissue engineering and regenerative medicine 14(3) (2017) 317-326.

[8] E.A. Huebner, S.M. Strittmatter, Axon regeneration in the peripheral and central nervous systems, Cell biology of the axon, Springer2009, pp. 305-360.

[9] M. Dadon-Nachum, O. Sadan, I. Srugo, E. Melamed, D. Offen, Differentiated mesenchymal stem cells for sciatic nerve injury, Stem Cell Reviews and Reports 7(3) (2011) 664-671.[10] P. Cuevas, F. Carceller, M. Dujovny, I. Garcia-Gómez, B.A. Cuevas, R. González-Corrochano, D. Diaz-González, D. Reimers, Peripheral nerve regeneration by bone marrow stromal cells, Neurological research 24(7) (2002) 634-638.

[11] J. Dodd, T.M. Jessell, Axon guidance and the patterning of neuronal projections in vertebrates, Science 242(4879) (1988) 692-699.

[12] W.T. Daly, L. Yao, M.T. Abu-rub, C. O'Connell, D.I. Zeugolis, A.J. Windebank, A.S. Pandit, The effect of intraluminal contact mediated guidance signals on axonal mismatch during peripheral nerve repair, Biomaterials 33(28) (2012) 6660-71.

[13] M. Senturk, M. Cakir, A. Tekin, T. Kucukkartallar, M.A. Yildirim, S. Alkan, S. Findik, Comparison of primary repair and repair with polyglycolic acid coated tube in recurrent laryngeal nerve cuts (an experimental study), Am J Surg (2019).

[14] S.H. Oh, J.R. Kim, G.B. Kwon, U. Namgung, K.S. Song, J.H. Lee, Effect of surface pore structure of nerve guide conduit on peripheral nerve regeneration, Tissue engineering. Part C, Methods 19(3) (2013) 233-43.

[15] Y. Hu, Y. Wu, Z. Gou, J. Tao, J. Zhang, Q. Liu, T. Kang, S. Jiang, S. Huang, J. He, S. Chen, Y. Du, M. Gou, 3D-engineering of Cellularized Conduits for Peripheral Nerve Regeneration, Sci Rep 6 (2016) 32184.

[16] W. Yu, J. Wang, J. Yin, Platelet-rich plasma: a promising product for treatment of peripheral nerve regeneration after nerve injury, Int J Neurosci 121(4) (2011) 176-80.

[17] L. Kucuk, H. Gunay, O. Erbas, U. Kucuk, F. Atamaz, E. Coskunol, Effects of platelet-rich plasma on nerve regeneration in a rat model, Acta Orthop Traumatol Turc 48(4) (2014) 449-54.

[18] H.H. Cho, S. Jang, S.C. Lee, H.S. Jeong, J.S. Park, J.Y. Han, K.H. Lee, Y.B. Cho, Effect of neural-induced mesenchymal stem cells and platelet-rich plasma on facial nerve regeneration in an acute nerve injury model, The Laryngoscope 120(5) (2010) 907-13.

[19] D. Sonnleitner, P. Huemer, D.Y. Sullivan, A simplified technique for producing platelet-rich plasma and platelet concentrate for intraoral bone grafting techniques: a technical note, The International journal of oral & maxillofacial implants 15(6) (2000) 879-82.

[20] C.H. Jo, Y.H. Roh, J.E. Kim, S. Shin, K.S. Yoon, Optimizing platelet-rich plasma gel formation by varying time and gravitational forces during centrifugation, Journal of Oral Implantology 39(5) (2013) 525-532.

[21] Y.T. Kim, V.K. Haftel, S. Kumar, R.V. Bellamkonda, The role of aligned polymer fiber-based constructs in the bridging of long peripheral nerve gaps, Biomaterials 29(21) (2008)

3117-27.

[22] L. Huang, L. Zhu, X. Shi, B. Xia, Z. Liu, S. Zhu, Y. Yang, T. Ma, P. Cheng, K. Luo, J. Huang, Z. Luo, A compound scaffold with uniform longitudinally oriented guidance cues and a porous sheath promotes peripheral nerve regeneration in vivo, Acta Biomater 68 (2018) 223-236.

[23] M. Sanchez, A. Garate, D. Delgado, S. Padilla, Platelet-rich plasma, an adjuvant biological therapy to assist peripheral nerve repair, Neural regeneration research 12(1) (2017) 47-52.

[24] J. Xiao, T.J. Kilpatrick, S.S. Murray, The role of neurotrophins in the regulation of myelin development, Neuro-Signals 17(4) (2009) 265-76.

[25] J. Qin, L. Wang, Y. Sun, X. Sun, C. Wen, M. Shahmoradi, Y. Zhou, Concentrated growth factor increases Schwann cell proliferation and neurotrophic factor secretion and promotes functional nerve recovery in vivo, International journal of molecular medicine 37(2) (2016) 493-500.

[26] J. Qin, L. Wang, L. Zheng, X. Zhou, Y. Zhang, T. Yang, Y. Zhou, Concentrated growth factor promotes Schwann cell migration partly through the integrin beta1-mediated activation of the focal adhesion kinase pathway, Int J Mol Med 37(5) (2016) 1363-70.

[27] R.H. Quarles, Myelin-associated glycoprotein (MAG): past, present and beyond, Journal of neurochemistry 100(6) (2007) 1431-48.

[28] P.H. Lopez, Role of myelin-associated glycoprotein (siglec-4a) in the nervous system, Advances in neurobiology 9 (2014) 245-62.

[29] J.M. Boggs, Myelin basic protein: a multifunctional protein, Cellular and molecular life sciences : CMLS 63(17) (2006) 1945-61.

[30] D.L. Yao, X. Liu, L.D. Hudson, H.D. Webster, Insulin-like growth factor I treatment reduces demyelination and up-regulates gene expression of myelin-related proteins in experimental autoimmune encephalomyelitis, Proceedings of the National Academy of Sciences of the United States of America 92(13) (1995) 6190-4.

[31] P.J. Apel, J. Ma, M. Callahan, C.N. Northam, T.B. Alton, W.E. Sonntag, Z. Li, Effect of locally delivered IGF-1 on nerve regeneration during aging: an experimental study in rats, Muscle & nerve 41(3) (2010) 335-41.

[32] S. Parrinello, I. Napoli, S. Ribeiro, P. Wingfield Digby, M. Fedorova, D.B. Parkinson, R.D. Doddrell, M. Nakayama, R.H. Adams, A.C. Lloyd, EphB signaling directs peripheral nerve regeneration through Sox2-dependent Schwann cell sorting, Cell 143(1) (2010) 145-55.
[33] D.W. Zochodne, The challenges and beauty of peripheral nerve regrowth, Journal of the peripheral nervous system : JPNS 17(1) (2012) 1-18.
[34] A. Ikumi, Y. Hara, T. Yoshioka, A. Kanamori, M. Yamazaki, Effect of local administration of platelet-rich plasma (PRP) on peripheral nerve regeneration: An experimental study in the rabbit model, Microsurgery 38(3) (2018) 300-309.

English abstract

Recurrent laryngeal nerve (RLN) damage during thyroidectomy results in vocal cord paralysis, which often leads to hoarseness, aspiration, and dyspnea and may even be life-threatening. We evaluated the usefulness of porous polycaprolactone (PCL) nerve guidance conduit (NGC) containing platelet rich plasma (PRP) for functional regeneration in a RLN injury in vivo and vitro. In vitro study, we evaluated human Schwann cells proliferation, migration and wound healing assay after treating PRP. RT PCR and Western were performed the expression of neurotrophic factors, myelin associated glycoprotein (MAG), and extracellular signal regulated kinases (ERK). In vivo study, We resected a 10-mm segment of left RLN in 22 New Zealand white rabbits and divided into two groups (n, pure NGC=10 vs. PRP loaded NGC =12). Vocal cord mobility was evaluated endoscopically at 8, 12, and 16 weeks after injury. Nerve growth through NGCs and vocalis muscle atrophy were assessed by H&E, and toluidine blue staining. Immunohistochemical stainings for acetylcholinesterase (AchE), anti-neurofilament (NF), and anti-S100 protein and transmission electron microscopy (TEM) were performed. At 16 weeks postoperatively, endoscopic evaluations showed significantly better nerve recovery in the PRP loaded NGC group than in the pure NGC group. PRP loaded group represented a significant higher area ratios of vocalis muscle than the pure PCL group. Histologically nerve growth from both nerve endings in the tube was more densely observed in the PRP loading NGC group compared to pure NGC group. The expressions of AchE, NF and S-100 in neural ending were significantly stronger in PRP loading NGC group than in pure NGC group. TEM imaging also showed more dense myelinated axons in PRP loaded group. In vitro study, the migration, wound healing and proliferation of Schwann cells increased in a PRP concentration dose-dependent manner. Neurotrophic factors in PRP increased Schwann cells proliferation and expression and secretion of neurotrophic factors by itself, and promoted functional recovery after peripheral nerve injuries in vivo. PRP loaded NGC provides a favorable environment for RLN regeneration, and it might be potential therapeutics for the regeneration of peripheral nerve.

Fig. 1. Schematic illustration. (A) NGC was filled with PRP, and activated PRP releases growth factors including neurotrophic factors. (B) The recurrent laryngeal nerves of rabbits were used for comparing the efficacy of pure NGC and PRP loaded NGC. NGC allowed to penetrate the oxygen and nutrients, not inflammatory cells.

Abbreviation: NGC, nerve guidance conduit; PRP, platelet rich plasma.

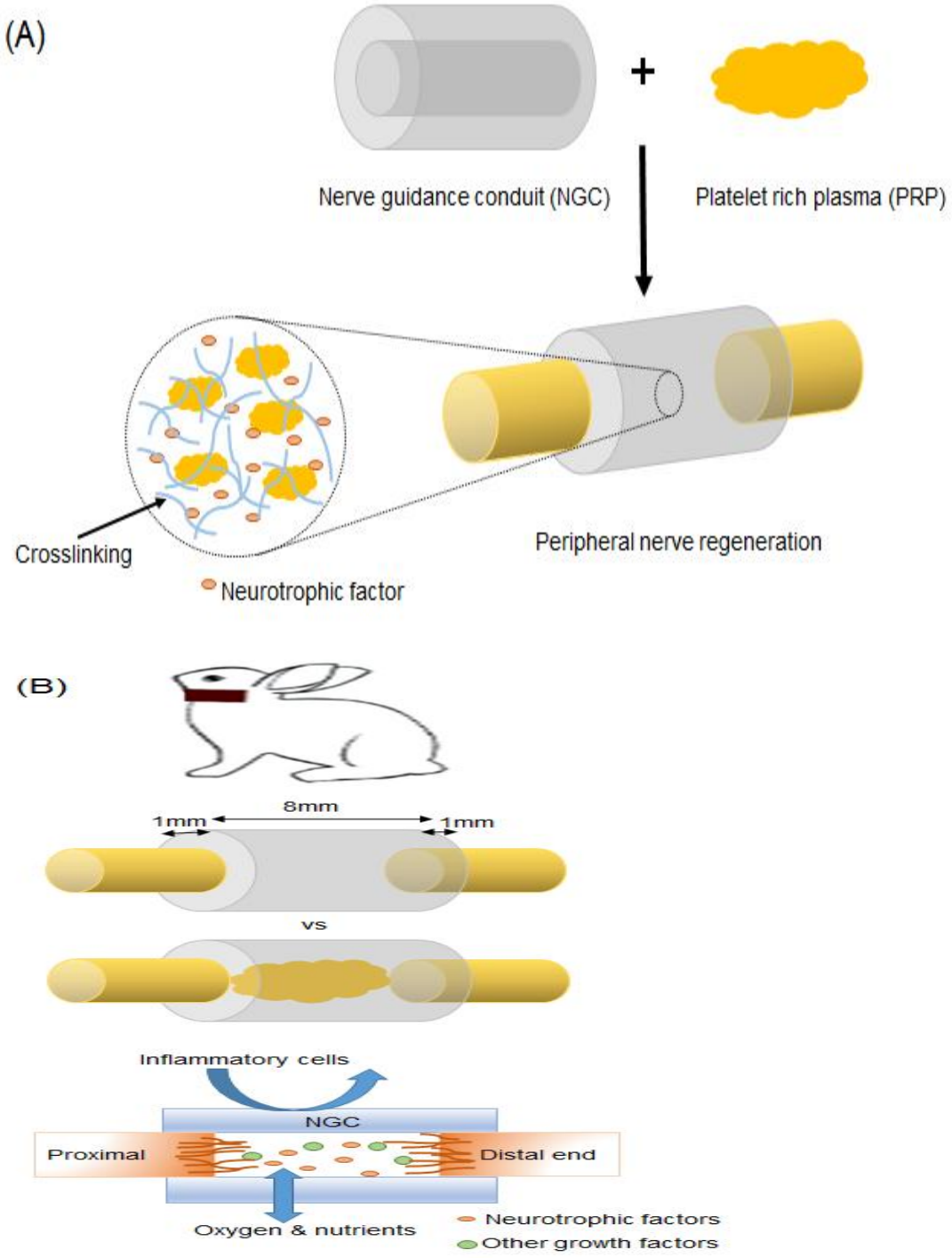

Fig. 2. Schematic illustration. (A) Axon was surrounded by myelin sheath, and Schwann cell which are located in myelin releases the neurotrophic factor. (B) PRP located in NGC stimulate to regenerate Schwann cells and axons by releasing neurotrophic factors. (C) Structure of MAG which may mediate interactions and signaling between myelin-forming cells and axons. MAG activates the extracellular signal regulated kinases 1 & 2 (ERK1/2) and phosphorylates neurofilaments leading to increase axonal caliber maintain and survive.

Abbreviation: NGC, nerve guidance conduit; PRP, platelet rich plasma; MAG, Myelin associated glycoprotein; ERK, extracellular-signal-regulated kinase protein.

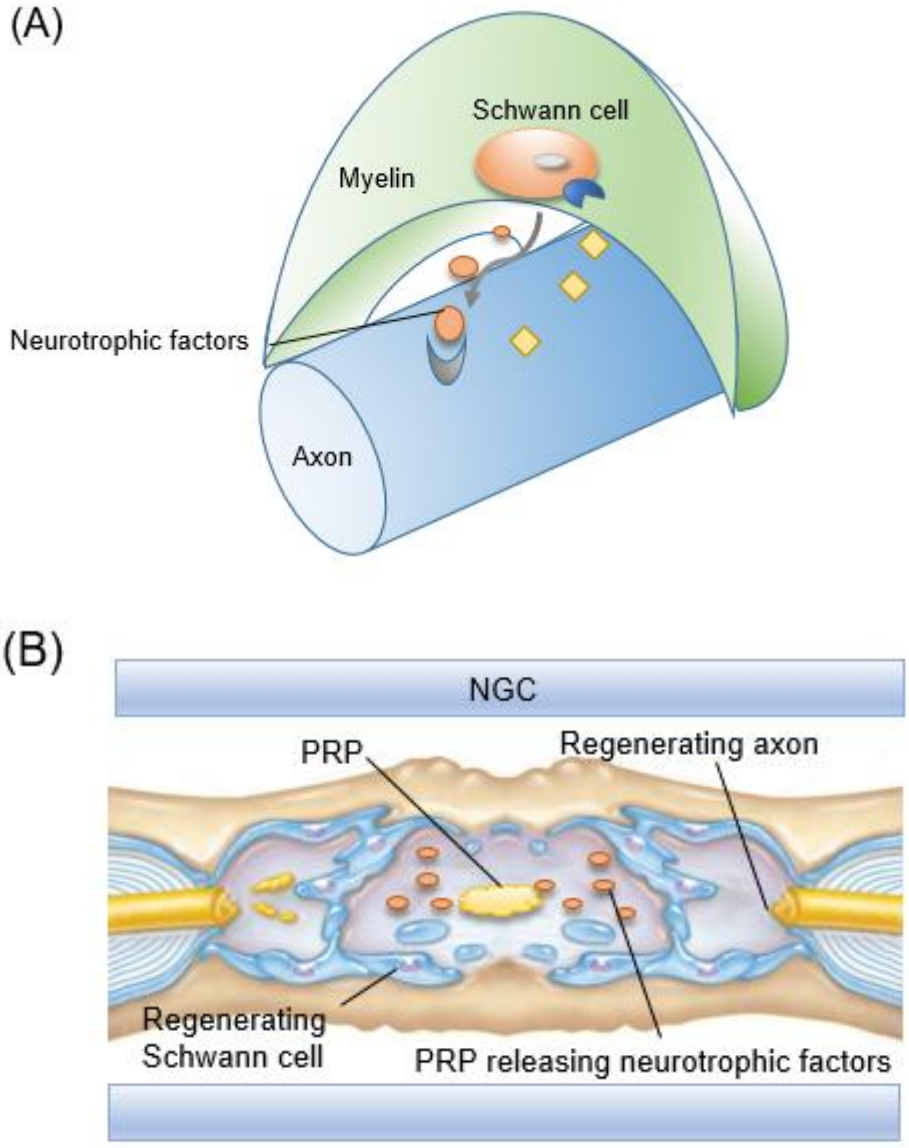

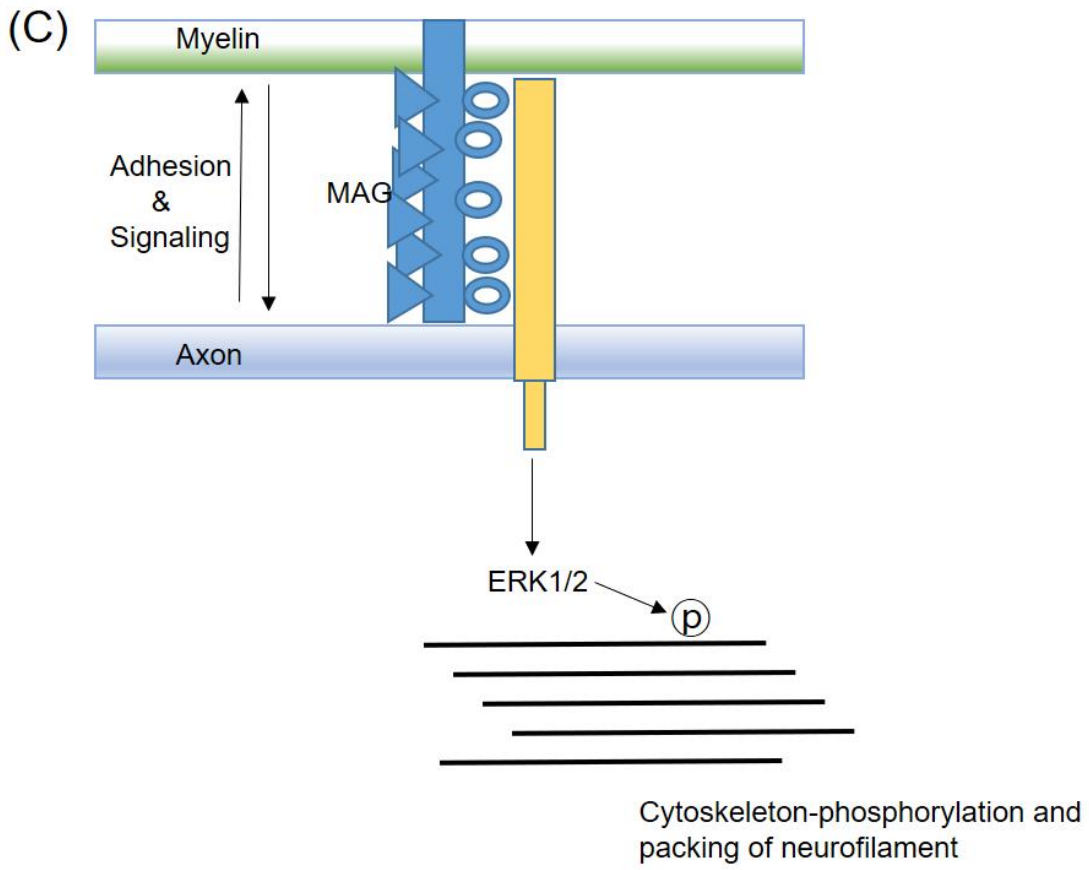
(C)
Myelin
Adhesion
&
Signaling
MAG
Axon
ERK1/2
p
Cytoskeleton-phosphorylation and
packing of neurofilament

Fig. 3. Interposition of the NGCs in a RLN injury animal model. (A) Schematic illustration of study design. (B) Photo of RLN (arrow) at experimental left side. (C) Photo of PCL/F127 NGC tube (arrow head).

Abbreviation: NGC, nerve guidance conduit; RLN, recurrent laryngeal nerve.

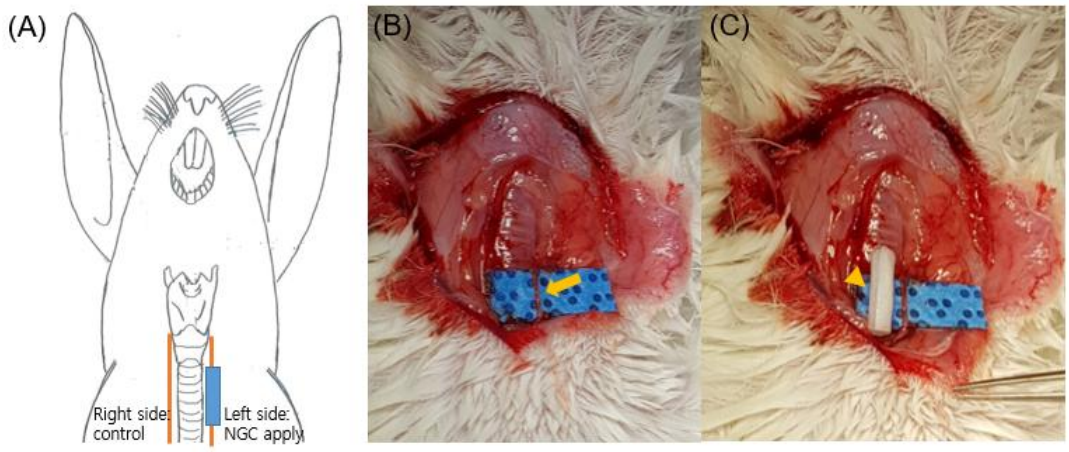

Fig. 4. The activation of PRP. (A) Detection of platelet activation marker CD62 by FACS. (B) On RT PCR, the level of TGF-β in activated state were significantly higher than resting state.(*, $P < 0.05$)

Abbreviation: PRP, platelet rich plasma; CD62, cluster of differentiation 62; FACS, Fluorescence-activated cell sorting; RT PCR, Reverse transcription polymerase chain reaction; TGF-β, Transforming growth factor beta.

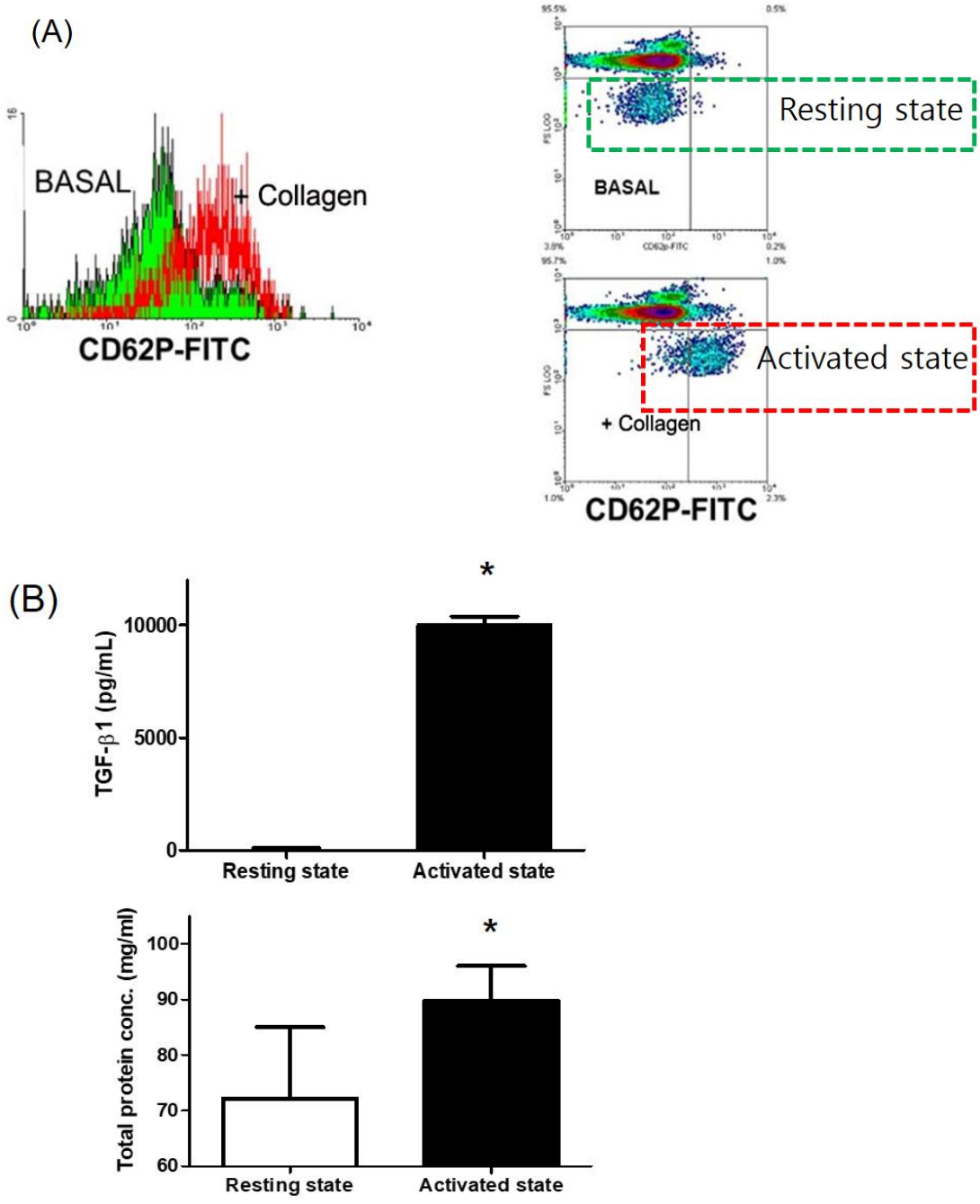

Fig.5. Analysis of the proliferation of hSCs. (A) hSCs showed spindle shaped and bipolar or occasionally multipolar cell morphology. As the dose of PRP increased, SCs showed higher proliferation rate. (B) The number of hSCs significantly increased in a PRP concentration by dose-dependent manner. At post treatment 96 hours, the cell count of hSCs under 10% PRP is statistically significant higher than the condition without PRP. (*, P = 0.001, by Kruskall Wallis test)

Abbreviation: hSCs, human Schwann cells; PRP, platelet rich plasma.

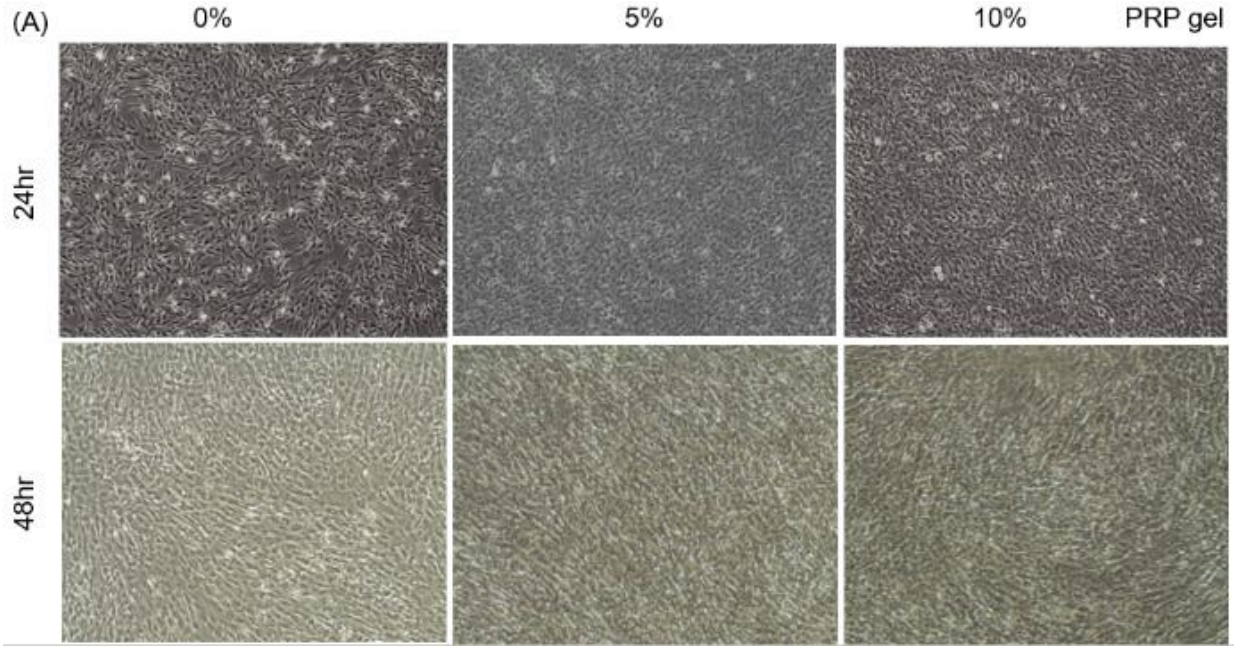

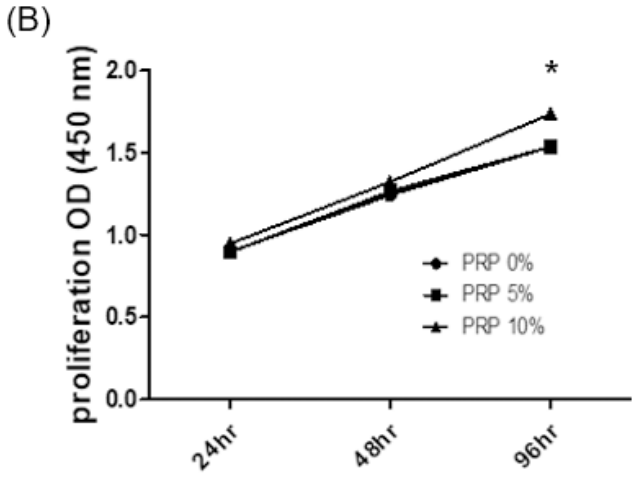

Fig.6 Transwell assay for hSCs migration. (A) Representative light photomicrographs of migrated hSCs induced by 0 and 5% PRP after 4 and 8 hour incubation. (B) While the hSCs in the 5% PRP substrates conditions demonstrated significantly faster cell proliferation rates than no PRP condition at post treatment 8 hours (*, $P = 0.043$)

Abbreviation: hSCs, human Schwann cells; PRP, platelet rich plasma.

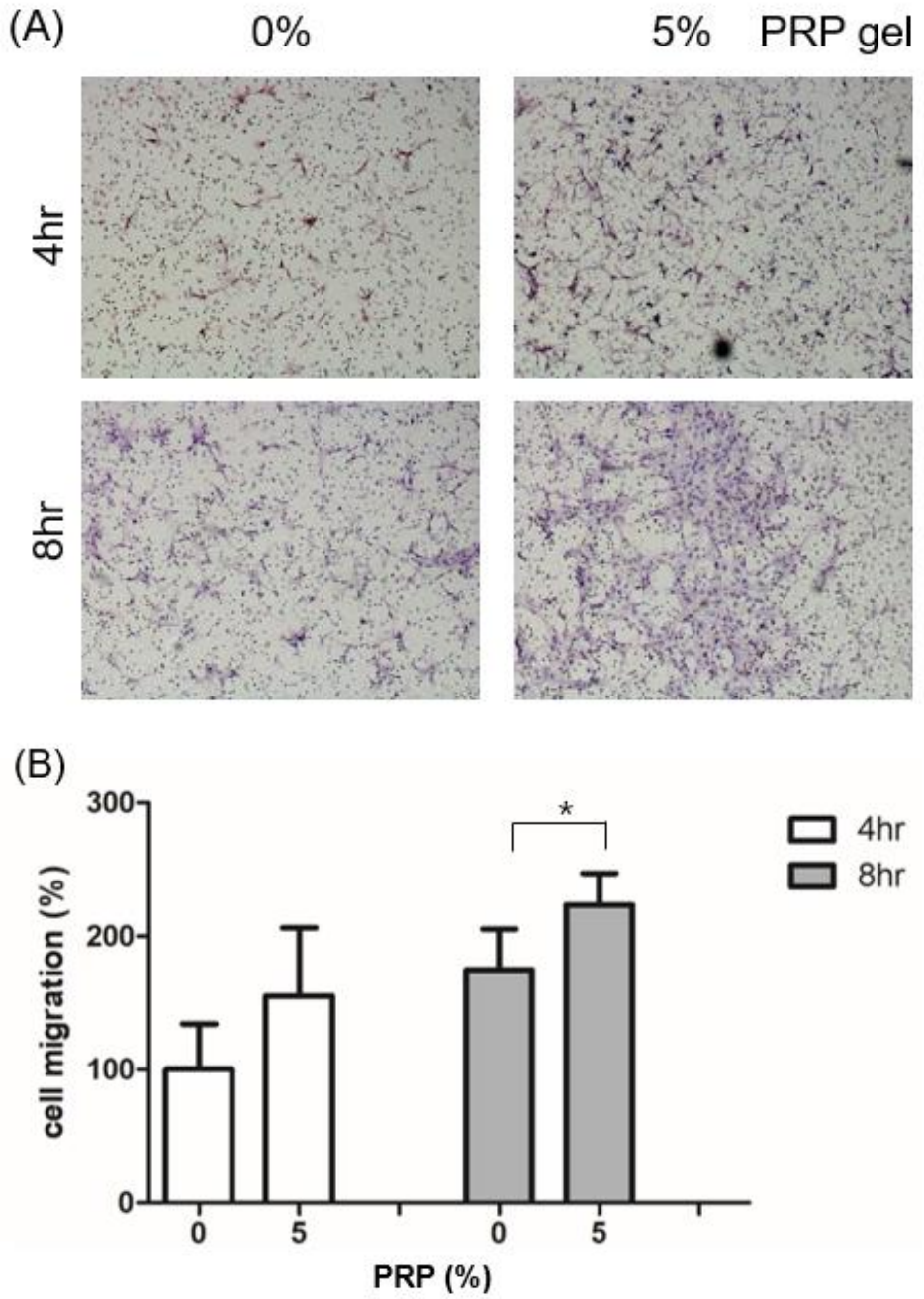

Fig.7. Analysis of the migration of hSCs. (A) Higher concentrated PRP treated hSCs significantly increased the migration rate in comparison with untreated SCs. The migration rate of the cells in the 10% PRP group was 4.25-fold greater than that of the cells without PRP group ($P < 0.05$).

Abbreviation: hSCs , human Schwann cells; PRP, platelet rich plasma.

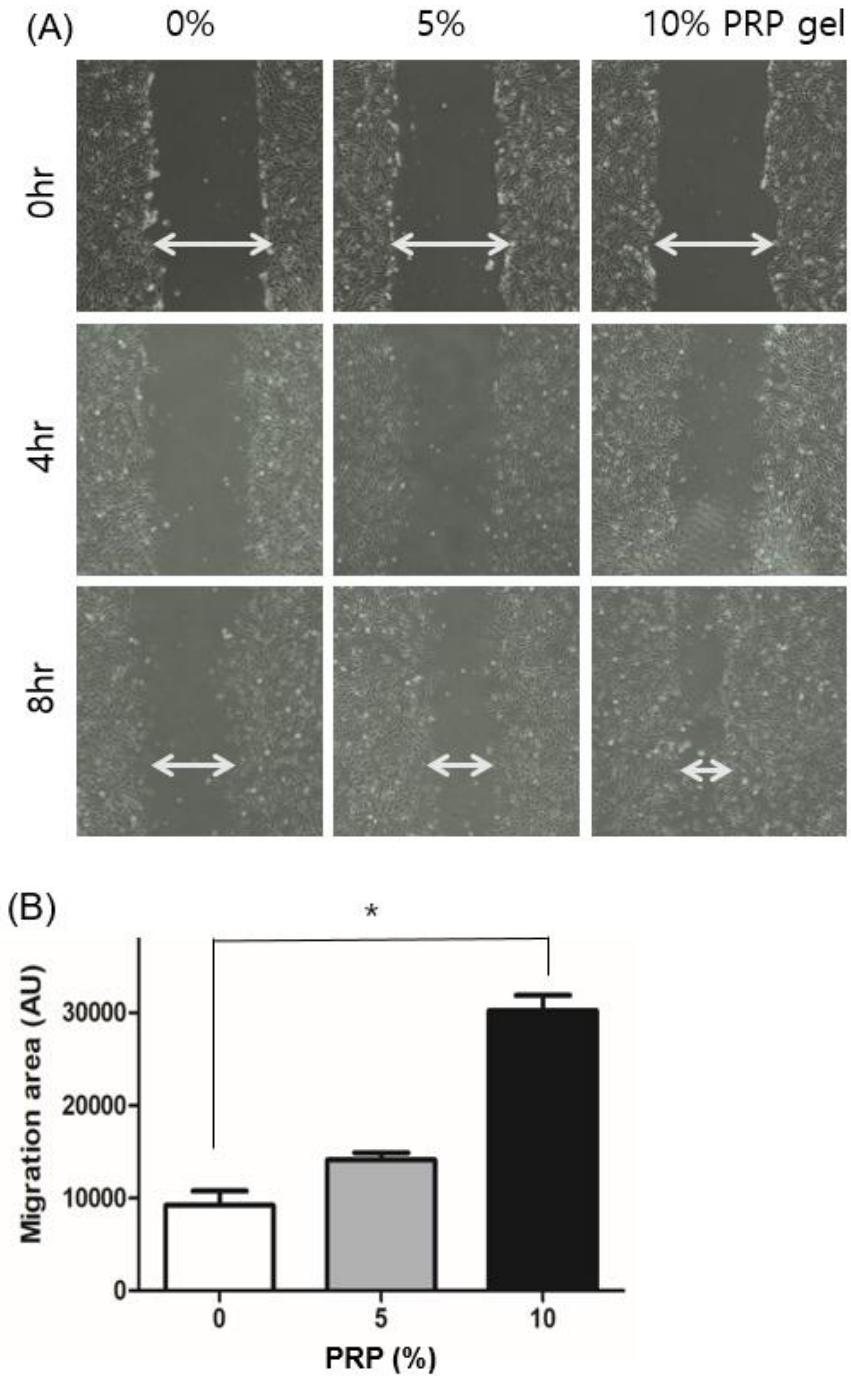

Fig.8. (A) Western blot analysis of neural regeneration related proteins in the condition of different concentration of PRP. (B) Quantification of neurotrophic factor including NT3 and NGF. As the concentration of PRP increase, the neurotrophic factors including NGF and NT-3 showed higher expression compared to the condition of no treatment. (C) Expression of MAG was increased by PRP with dose dependent manner. ERK, which is the MAG related axon cytoskeleton proteins, also showed the higher expression when the PRP is administered. (D) The expression of NGF from hSC by human ELISA, hSCs have expressed the NGF in a PRP dose dependent manner.

Abbreviation: PRP, platelet rich plasma; NGF, nerve growth factor; NT-3, neurotrophin-3; MAG, Myelin-associated glycoprotein; MBP, Myelin basic protein; ERK, extracellular-signal-regulated kinase protein.

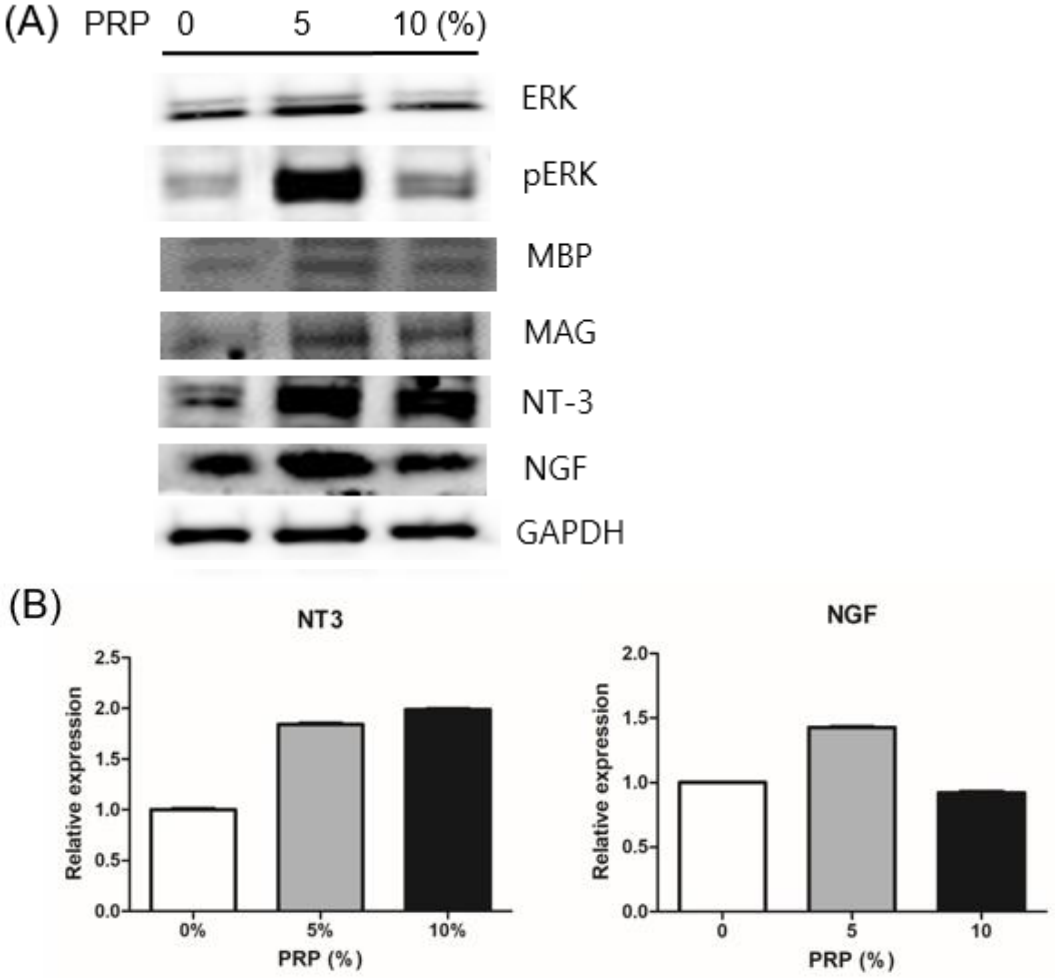

(C)

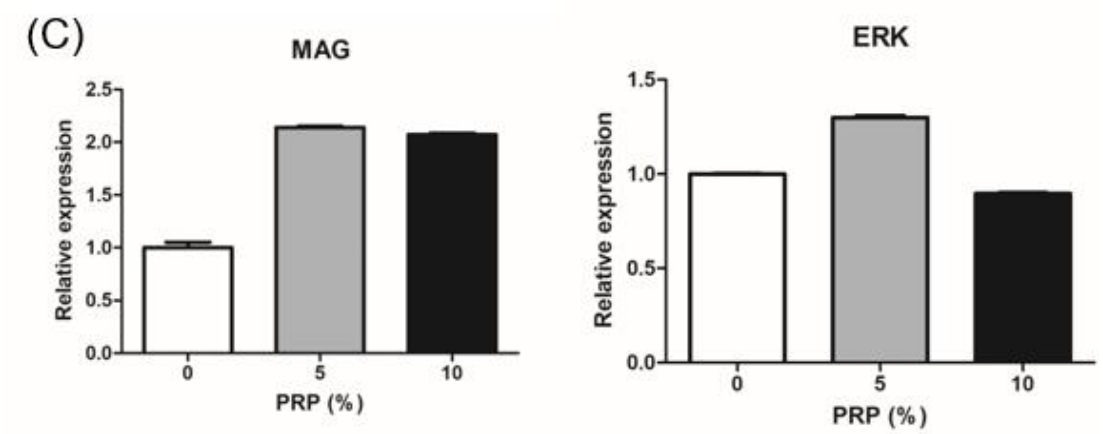
MAG
Relative expression
2.5
2.0
1.5
1.0
0.5
0.0
0
5
10
PRP (%)
ERK
Relative expression
1.5
1.0
0.5
0.0
0
5
10
PRP (%)

(D)

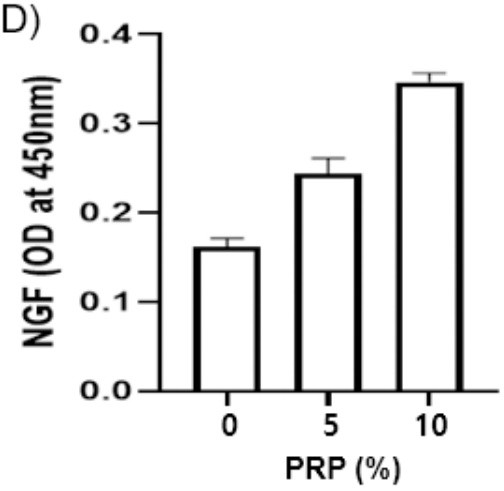
NGF (OD at 450nm)
0.4
0.3
0.2
0.1
0.0
0
5
10
PRP (%)

Fig.9. Endoscopic examinations of vocal cord movement and histologic analysis of target muscle (vocalis muscle) (A) Captured images of adducted position after nerve stimulation and abducted position. (B) The relative gap ratios between vocal cord adduction and abduction showed significantly higher gap ratio in PRP loaded NGC group (80.23 ± 6.91%) compared to the pure NGC group (48.99 ± 10.71%) (P = 0.018) (C) Axial section of vocalis muscle, PRP group showed similar muscle thickness at both side, but pure NGC group showed atrophied muscle at left side vocal cord. (D) On quantification analysis, PRP loaded NGC group represented a significant higher area ratios of vocalis muscle than the pure PCL group at postoperative 12 weeks (P = 0.033).

Abbreviation: NGC, nerve guidance conduit; PRP, platelet rich plasma

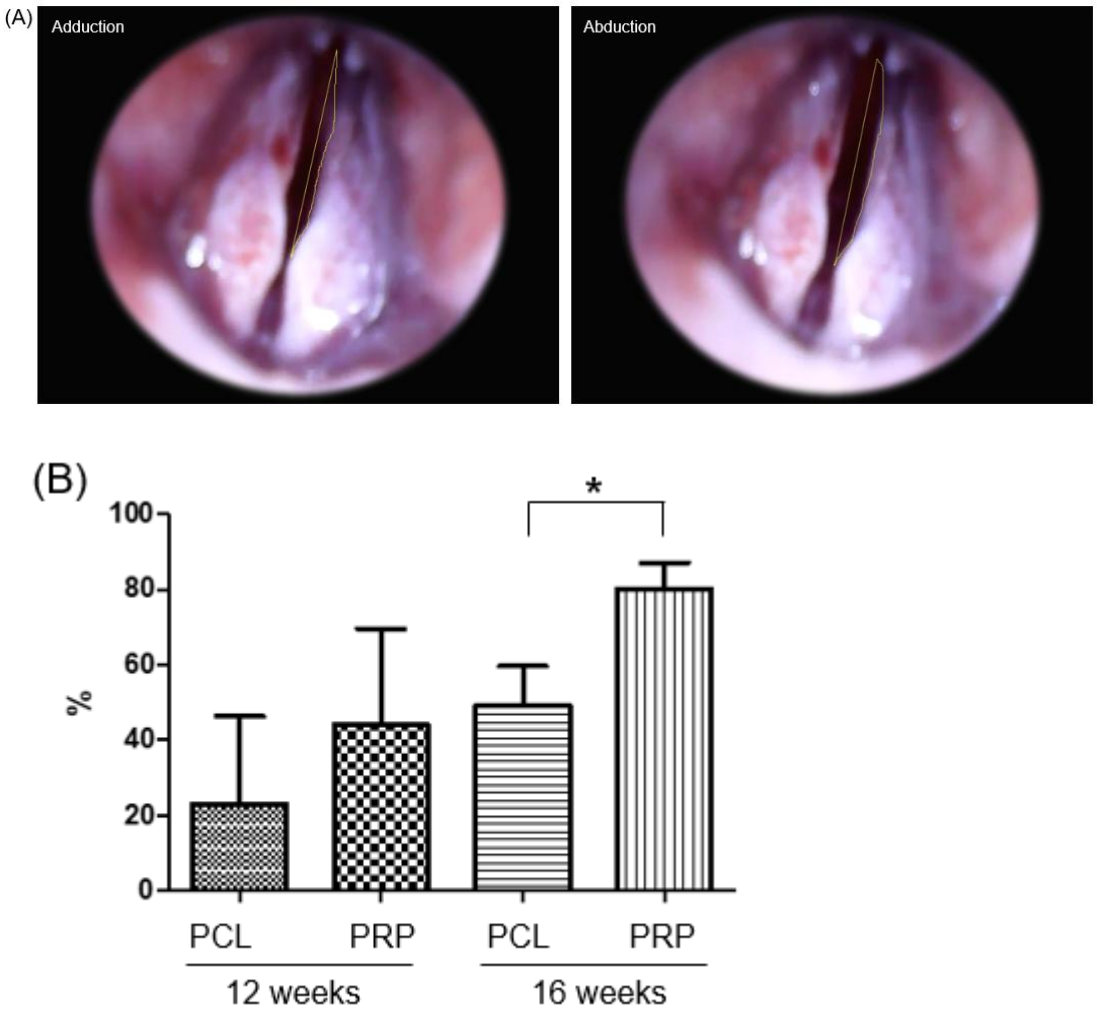

(C)

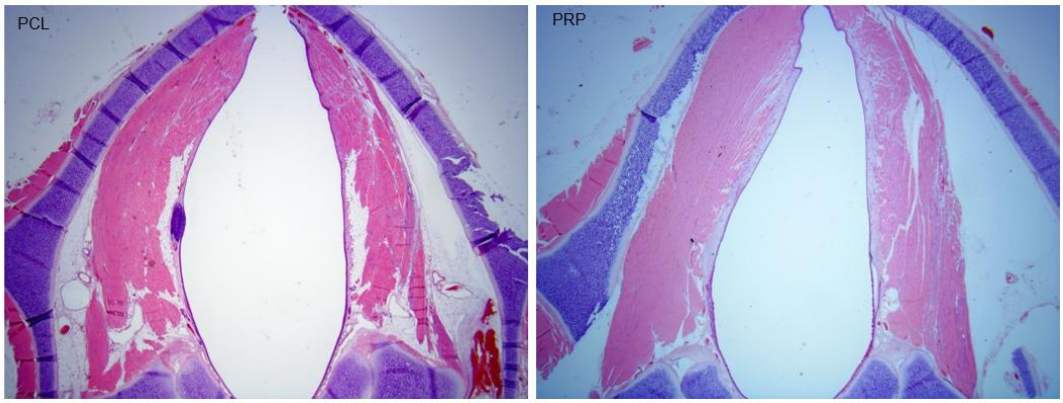

(D)

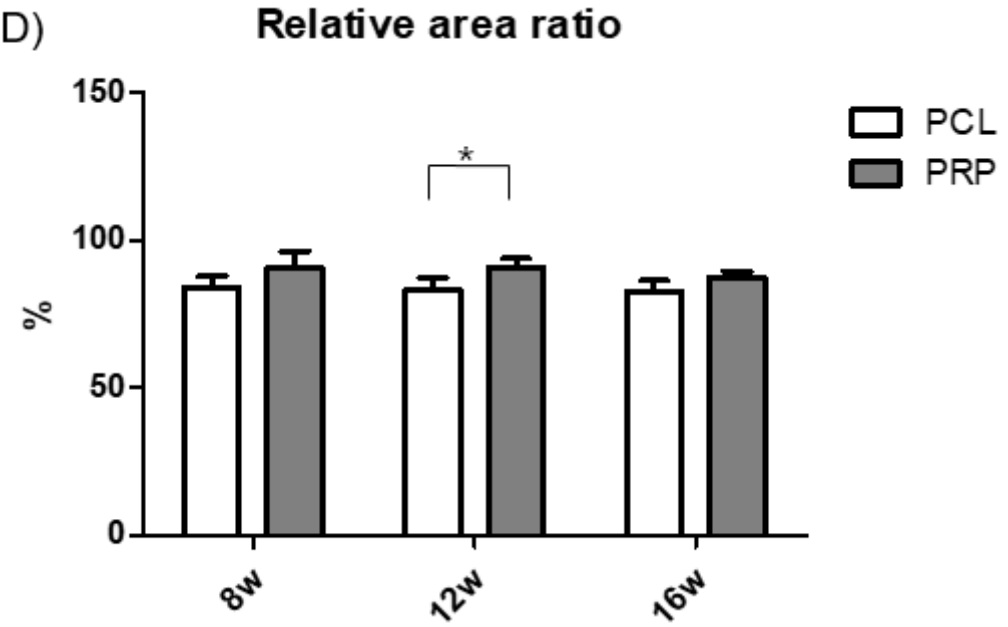

Fig. 10. Histologic evaluation (H&E and toluidine blue staining) and immunohistochemistry analysis of regenerated RLNs. (A) Longitudinal sections along with RLN at sixteen weeks postimplantation showed gradual nerve growing within NGC. Nerve budding from each side are connected at 16 weeks in PRP loaded NGC group (B) Immmunohistochemistry analysis by NF, S100 and AchE at sixteen weeks postimplantation showed strong positive in PRP loaded NGC group compared to pure NGC.

Abbreviation: H&E, hematoxylin and eosin staining; RLN, recurrent laryngeal nerve; NGC, nerve guidance conduit; PRP, platelet rich plasma; NF, Neurofilaments; S100, S100 protein; AchE, acetylcholinesterase.

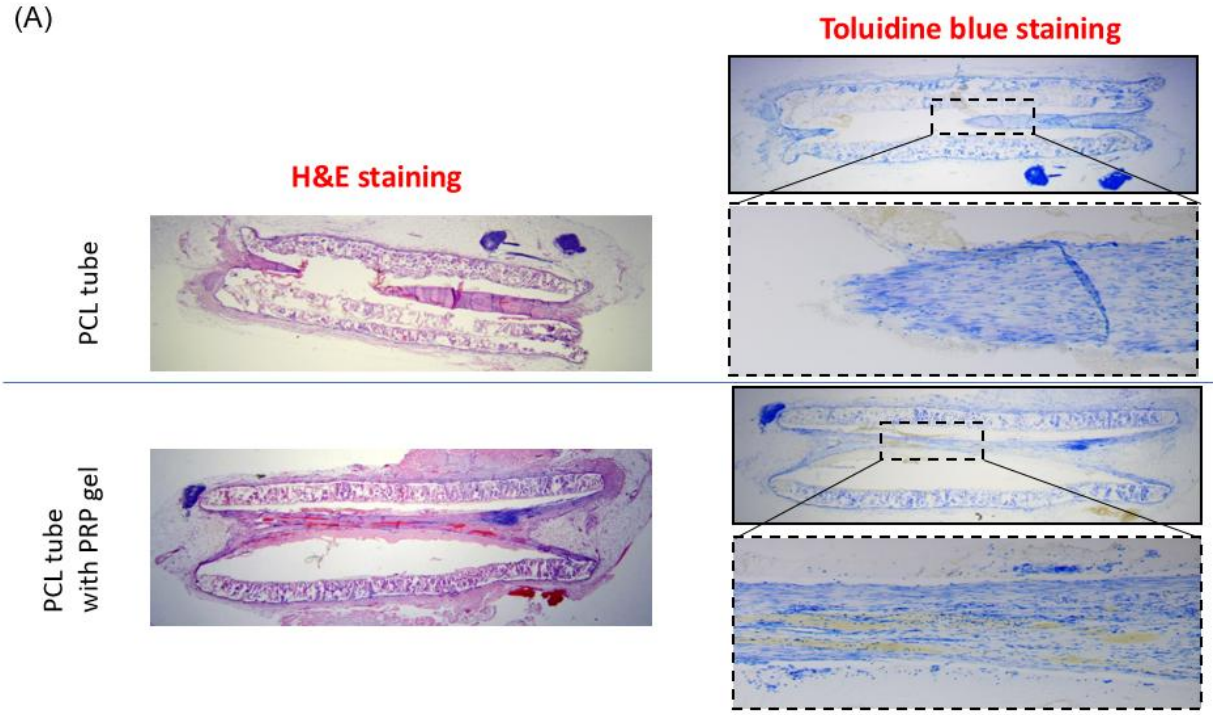

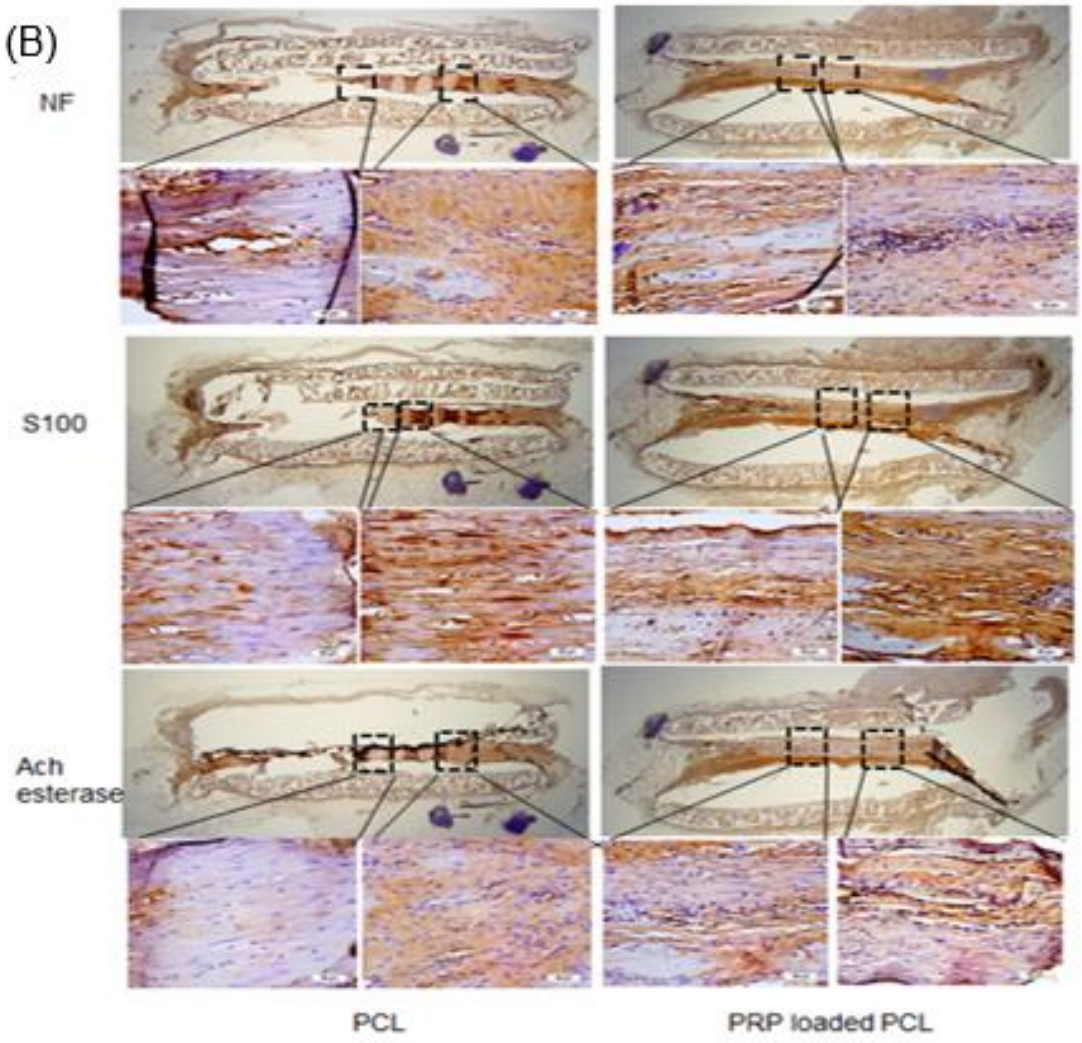
(B)
NF
S100
Ach esterase
PCL
PRP loaded PCL

Fig.11. Transmission electron microscopy (TEM) findings at eight and sixteen weeks postimplantation. More abundant myelinated fiber formation than pure NGC group. The structure of the axon fibers in the PRP loaded NGC group at sixteen weeks showed more dense and well organized with Schwann cells than eight weeks results. (A) TEM image at eight weeks postimplataion (B) TEM images at sixteen weeks after procedure.

Abbreviation: NGC, nerve guidance conduit; PRP, platelet rich plasma.